arXiv:1604.03719v2 [astro-ph.HE] 14 Apr 2016

The Equatorial Current Sheet and other interesting features of the Pulsar Magnetosphere

Ioannis Contopoulos[1,2]†

[1]Research Center for Astronomy and Applied Mathematics, Academy of Athens
4 Soranou Efessiou Str., Athens 11527, Greece

[2]National Research Nuclear University, 31 Kashirskoe highway, Moscow 115409, Russia

(Received ; revised ; accepted .)

We want to understand what drives magnetospheric dissipation in the equatorial current sheet. Numerical simulations have limitations and, unless we have a clear a priori understanding of the physical processes involved, their results can be misleading. We argue that the canonical pulsar magnetosphere is strongly dissipative and that a large fraction (up to $30-40\%$ in an aligned rotator) of the spindown luminosity is redirected towards the equator where it is dissipated into particle acceleration and emission of radiation. We show that this is due to the failure of the equatorial electric current to cross the Y-point at the tip of the corotating zone.

PACS codes:

1. Limitations of numerical simulations

Numerical simulations help us understand how real pulsars work. Unfortunately, they have severe limitations:

1.1. *Lego^{TM} tiles*

The radius of a neutron star is about 10km. The light cylinder lies a few to a few thousand times away. The polar cap is a few to a hundred times smaller. It is thus very hard to equally resolve in 3D the stellar vicinity and the magnetosphere over several light cylinder radii, with the possible exception of millisecond pulsars. The current state-of-the-art 3D numerical resolution consists of at most a few hundred grid cells in each direction inside the light cylinder. This is manifestly insufficient to capture and resolve certain important features of the pulsar magnetosphere that are seen in high-resolution 2D solutions. Ten years ago, Timokhin (2006) analyzed the axisymmetric pulsar magnetosphere in the highest yet achieved resolution of more than 10,000 grid cells inside the light cylinder. Even though that resolution is not sufficient to resolve the internal structure of the current sheet, it taught us a couple of interesting things about the magnetospheric Y-point (the tip of the corotating -so called 'dead'- zone) that are hard to see in 3D simualtions:

(a) The poloidal magnetic and electric fields right above and below the Y-point both drop to zero. Thus, the charge density at the Y-point also drops to zero (see also Uzdensky 2003).

† Email address for correspondence: icontop@academyofathens.gr

(*b*) In the ideal MHD solution (Contopoulos *et al.* 1999, hereafter CKF), the current sheet extends inwards of the Y-point along the boundary (separatrix) of the dead zone. In that region, the current sheet is charged oppositely to the charge of the equatorial current sheet, and its charge density changes discontinuously to zero at the Y-point. In particular, as the Y-point approaches the light cylinder, the electric and magnetic fields and the charge density right interior to it diverge (Uzdensky 2003; Kalapotharakos & Contopoulos 2009).

These features of the current sheet are completely lost in current 3D numerical simulations. What is most disconcerning, is that in order to determine the pulsar energy losses, i.e. its spindown rate, we need to know the position of the Y-point since this is what determines how many field lines remain closed in the dead zone, and how many carry electromagnetic radiation. In numerical simulations that begin with a stationary star that is then set to uniform rotation, it has been observed that magnetic field lines open up after a fraction of one stellar rotation and a Y-point forms initially at some distance $r_{\rm Y}$ *inside* the light cylinder (the cylindrical radius $r_{\rm LC} \equiv c/\Omega$, where Ω is the stellar rotational angular velocity). When that happens, the solution settles to a perfectly valid ('happy') steady-state that emits electromagnetic energy at a rate $L(r_{\rm Y}) \approx (r_{\rm Y}/r_{\rm LC})^{-2} L(r_{\rm LC}) > L(r_{\rm LC})$ (see also Contopoulos 2005; Timokhin 2006). The Y-point then gradually evolves towards the final steady state where the Y-point reaches the light cylinder. Depending on the numerical resolution, that evolution takes place at a much longer timescale (several rotational periods) than the timescale (fraction of one period) needed for the original happy steady-state to establish itself. Notice that in practice, the Y-point is determined as the innermost tip of the equatorial current sheet where it reaches the corotating dead zone.

This may very well be a serious problem in the numerical determination of the pulsar spindown rate. What we are really interested to know is $L(r_{\rm LC})$ because we believe that as the pulsar spins down, the corotating dead zone manages to always lie close to the instantaneous light cylinder, thus $r_{\rm Y} \approx r_{\rm LC}$. This is achieved via continuous reconnection at the Y-point through which more and more formerly open field lines close and increase the size of the dead zone. If that is not the case, and during the small amount of time available to run our numerical simulation the magnetosphere has relaxed to an $r_{\rm Y}$ significantly different from $r_{\rm LC}$ (see Fig. 1; compare also to Fig. 3 of Philippov *et al.* 2015), then the numerical estimate of the spindown luminosity $L(r_{\rm LC})$ is unreliable. Notice that in reality, $r_{\rm Y}$ may not keep up with the light cylinder as the pulsar spins down, and this may account for the measured values of pulsar braking indices that are found to be less than the canonical value of 3 (see also Kundt 1998, for an alternative view). The numerical evaluation of the real pulsar braking index is, however, way beyond the capabilities of modern computers.

1.2. *Death Stars*^{TM}

In Hollywood fiction, Death Stars$^{\rm TM}$ shoot intense beams of energy on their own. Real pulsars work differently. A certain magnetospheric structure is established that *demands* a certain flow of charged particles through it in order to support the so-called Goldreich-Julian electric charge density $\rho_{\rm GJ}$ (Goldreich & Julian 1969) and the CKF electric current density $J_{\rm CKF}$ throughout (the first time this name was used was in Contopoulos & Kalapotharakos 2010). There is a clear distinction here between the so-called Goldreich-Julian electric current density defined as $J_{\rm GJ} \equiv \rho_{\rm GJ} c$ in the overall outward direction along magnetic field lines, and the actual electric current density $J_{\rm CKF}$ that is required throughout the magnetosphere in order to establish a force-free ideal MHD equilibrium. In general, $J_{\rm CKF}$ has nothing to do with $J_{\rm GJ}$, except in the asymptotic region $r \gg r_{\rm LC}$

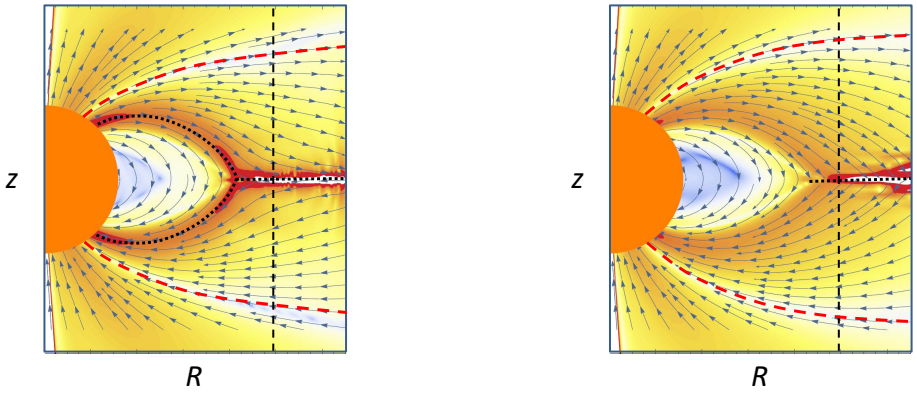

FIGURE 1. Examples of ideal MHD numerical simulations with Y-points clearly inside the light cylinder. These particular simulations run only for 6 stellar rotations which apparently wasn't enough time for them to relax to a final steady state. Vertical dashed line: line cylinder. Lines with arrows: poloidal magnetic field. Color scale: magnitude of poloidal electric current density multiplied by R^2 (white regions: no poloidal currents; red regions: poloidal current sheets, also drawn with black dotted lines). The lines of zero poloidal electric current that separate the regions of outgoing and ingoing electric currents are shown with red short dashed lines (see also Fig. 2). Orange semicircle: neutron star. Left: E is enforced to be less than B everywhere. In practice, this implies that current sheets are treated as contact discontinuities. Both the equatorial and separatrix current sheets form. The equatorial current sheet extends clearly inside the light cylinder. The current sheet appearing inside the Y-point is clearly an artifact of our particular treatment of contact disctontinuities. Right: We allow E to take any value compared to B, and current sheets are treated with a dissipative Aristotelian prescription (Gruzinov 2013). In that case, only the equatorial current sheet survives, and the separatrix current sheet disappears, as expected in Contopoulos *et al.* (2014), and seen also very clearly in Fig. 3 of Cerutti *et al.* (2015*a*).

where $J_{\rm CKF} \to J_{\rm GJ}$. CKF were the first to argue that the establishment of this particular electric current distribution is *as important* for the global solution *as* the establishment of the well known Goldreich-Julian electric charge distribution.

How the magnetosphere achieves this configuration (i.e. what is the particular type, distribution, and kinematics of the charge carriers that fill the magnetosphere) remains a matter of active research and disagreement (see section 4 below). There seems to exist several (an infinity?) ways to achieve a happy configuration, and Nature decides which one to establish, but one thing is certain: the star does not shoot charged particles on its own. We are concerned about the results of numerical simulations because whenever the density drops below a limit that a code cannot handle (a so called 'density floor'), the code freely supplies matter in the 'problematic' regions. It is often seen that the value of the density floor or the particle replenishment rate affect the outcome of the numerical evolution (Philippov *et al.* 2015). Even if such floors do exist in nature in the form of microscopic processes that e.g. freely generate electron-positron pairs wherever they are needed (e.g. Chen & Beloborodov 2014), their values are more than twenty orders of magnitude beyond the capabilities of modern supercomputers in a global magnetospheric simulation. Indeed, the most recent calculations contain about 10^8 particles over a volume on the order of $r_{\rm LC}^3$ and reach sigma values on the order of 10^4. Assuming a neutron star magnetic field on the order of 10^{12} G, this corresponds to particles with charge and mass more than twenty orders of magnitude larger than the charge and mass of the electron, and number densities more than twenty orders of magnitude smaller than the corresponding Goldreich-Julian densities at the light cylinder.

We believe that global numerical simulations cannot yet teach us what is the type of charge carrier that fills the magnetosphere, and where are these particles generated. It

is too early for an ab initio reconstruction of the pulsar magnetosphere, and we need to return to our drawing boards and reconsider the global picture.

1.3. *Trade secrets*

We would like to acknowledge a danger with time dependent ideal MHD numerical simulations in their treatment of current sheets. A current sheet obviously lies outside the regime of ideal MHD, so, mathematically, it should be treated as an unresolved contact discontinuity. Obviously, numerical codes encounter problems at the locations where the current sheet begins to form. These problems are treated with special custom techniques developed by each programer for his/her own code (the 'trade secrets'). In particular, how $\mathbf{E} \cdot \mathbf{B} = 0$ is enforced, and how we make sure that E nowhere exceeds B (in ideal MHD) yield a particular time dependent evolution in each particular code. The important goal of course is for all different codes to be able to reproduce the gross features of the final steady state obtained by CKF and described in extreme detail by Timokhin (2006). Different codes yield slightly different results regarding the detailed structure around the current sheet (e.g. oppositely charged layers above and below the equatorial current sheet seen in Contopoulos & Kalapotharakos 2010; Kalapotharakos *et al.* 2012, , a current sheet right inside the Y-point as seen in Fig. 1, etc.). Unfortunately, there exist few high resolution test solutions and all of them are axisymmetric and steady-state.

The message we want to convey here is that existing numerical codes have been 'tweaked' to reproduce the magnetospheric current sheets appearing in the few known axisymmetric ideal MHD solutions available in the literature. Currently there are no 3D tests of 3D codes. Most importantly though, because of their particular 'tweaks', we cannot yet trust their time-dependent evolution in more sophisticated simulations like evolving binary neutron star magnetospheres. This may potentially be problematic in the numerical simulations of the transient electromagnetic signal expected when two magnetospheres colide during the merger of two neutron stars or two black holes (e.g. Baker *et al.* 2013; Ponce *et al.* 2014).

2. What drives magnetospheric dissipation?

Let us remind the reader how we arrived at our current understanding of the pulsar magnetosphere. The basic picture of a unipolar inductor was formulated by Goldreich & Julian (1969) and a cartoon of the magnetospheric structure was drawn. In that picture, electric charges fill and electric currents flow through the magnetosphere, in such a way that an outward $\mathbf{E} \times \mathbf{B}$ Poynting flux vector develops everywhere. Another fact that was obvious from the very first discussion on pulsar magnetospheres is that the magnetosphere, if ideal, must open up beyond a distance from the axis of rotation known as the light cylinder. Obviously, a poloidal magnetic field discontinuity must inevitably form beyond the light cylinder (as is shown in the original Goldreich-Julian cartoon), but that is not too important since the poloidal magnetic field drops very fast with distance from the light cylinder.

What is much more important is an equatorial discontinuity in the azimuthal magnetic field, i.e. the existence of an equatorial *poloidal* current sheet. The first who theorized this configuration was Lyubarskii (1990), and this led to a very important school of thought that the acceleration of the pulsar wind may in fact take place in the equatorial poloidal current sheet (Lyubarsky & Kirk 2001). However, his original argument for the existence of such a current sheet was based on a study of an artificial solution up to (and *not* beyond) the light cylinder consisting of field lines that close some distance inside the light cylinder, and field lines that reach the light cylinder. Obviously, at that time it was

completely uncertain what the latter field lines would do beyond the light cylinder, and unless a global solution was obtained, no one was in a position to know with confidence whether such an equatorial *poloidal* current sheet existed or not.

That solution appeared 30 years later (CKF) and was for several years met with caution and disbelief (Ogura & Kojima 2003). Current sheets are usually unstable in nature, so the equatorial current sheet that CKF obtained was thought to be artificial. A few authors tried to refute our discovery proposing various other solutions without current sheets, but all such efforts did not seem to represent real pulsar magnetospheres (Lovelace *et al.* 2006; Beskin 2010). Only after Spitkovsky (2006) reproduced our solution as the final steady-state (after twenty rotations) of a time-dependent numerical evolution did the community begin to pay attention to the possibility that the equatorial poloidal current sheet discovered by CKF may be an integral and most important part of the pulsar magnetosphere. Spitkovky's numerical results have since then been confirmed by several others (McKinney 2006; Kalapotharakos & Contopoulos 2009; Tchekhovskoy *et al.* 2013).

However difficult the numerical problems associated with the equatorial current sheet may be (see previous section), we cannot ignore it. An important point that we tried to emphasize during a series of 3 short papers that we wrote many years ago (Contopoulos 2007*a*,*b*,*c*) is that one cannot say anything about pulsars without taking proper account of the equatorial current sheet. As we argued in the previous section, pulsars do not shoot energetic beams on their own. Pulsar magnetospheres are global structures that are characterized by what happens both on the surface of the star (the magnetic field structure, the rotation rate, and the availability or non-availability of charge carriers there), and at the equatorial current sheet that develops way out in the magnetosphere, *and not* by the boundary conditions at 'infinity' (as long as the system is able to establish super Alfvènic radiation conditions ($\mathbf{E}\times\mathbf{B}/B^2\to\hat{\mathbf{r}}$ at large distances). In particular, if the physical conditions in the current sheet preclude any dissipation there, the current sheet establishes itself as a contact discontinuity with $\mathbf{B}$ parallel to it above and below it. This was the case for CKF and all subsequent ideal MHD simulations. Physically, this implies that the magnetosphere is able to supply the electric charge carriers needed to support the electric charge density and electric current density required by the ideal MHD solution. As long as the required charges are freely supplied, there is no 'residual' electric field along the current sheet that would lead to particle acceleration along the current sheet and/or reconnection.

At this point, we would like to describe briefly what takes place along the equatorial current sheet. As we said, in a contact discontinuity the magnetic field is parallel to it above (let as denote it with $\mathbf{B}_{\parallel\mathrm{CS}}$), reverses direction inside the current sheet, and becomes equal in magnitude and antiparallel below. At the same time, the electric field is perpendicular to it above the current sheet (let us denote it with $\mathbf{E}_{\perp\mathrm{CS}}$), reverses direction and points in the opposite perpendicular direction below, thus the current sheet is obviously charged with surface electric charge density

$$\sigma=\frac{E_{\perp\mathrm{CS}}}{2\pi}\ . \tag{2.1}$$

Notice that $E_{\perp\mathrm{CS}}=(r/r_{\mathrm{LC}})B_r$ above the current sheet. In this picture, there is no 'residual' electric field *along* the current sheet. Such a field component (let us denote it with $\mathbf{E}_{\parallel\mathrm{CS}}$) would appear only if the magnetosphere above and below the current sheet is *driven* to converge towards it with convergence velocity

$$v_{\mathrm{converge}}\equiv\frac{\mathbf{E}_{\parallel\mathrm{CS}}\times\mathbf{B}_{\parallel\mathrm{CS}}}{B^2}c\ . \tag{2.2}$$

Notice that $\mathbf{E}_{\parallel \rm CS}$ lies along the direction of the electric current in the current sheet, hence it is perpendicular to $\mathbf{B}_{\parallel \rm CS}$, and continuous (in the same direction) above and below the current sheet ($\mathbf{E}_{\parallel \rm CS}$ becomes radial, $\parallel \hat{\mathbf{r}}$, in the current sheet midplane). This is often called the reconnection electric field, and in the ideal MHD region right above and below the current sheet, $E_{\parallel \rm CS} = (r/r_{\rm LC})B_z$. Why this is nonzero depends of course on the global structure of the magnetosphere. On the other hand, this is what dictates the dissipation rate at the current sheet, which is obviously related to the microscopic conditions in the current sheet. So the 'chicken and egg' question is:

What drives the dissipation at the current sheet?

Is it the global magnetospheric structure that redirects electromagnetic Poynting flux towards the equator, or the local reconnection and plasma acceleration that dissipates energy in the current sheet?

In a steady state, a balance will be achieved between the Poynting flux $\mathbf{E}_{\parallel \rm CS} \times \mathbf{B}_{\parallel \rm CS}$ entering the current sheet and the effective dissipation rate $\eta E^2_{\parallel \rm CS}$ in the current sheet (we have defined here an effective dissipation parameter η such that $J_{\rm CS} = E_{\parallel \rm CS}/\eta$). Thus, the residual electric field in the current sheet is equal to

$$E_{\parallel \rm CS} = \frac{2\eta}{lc} B_{\parallel \rm CS} \equiv \frac{2}{\mathcal{R}_{\rm m}} B_{\parallel \rm CS}, \tag{2.3}$$

where, l is the thickness of the current sheet, and $\mathcal{R}_{\rm m}$ is the associated magnetic Reynolds number (or Lundquist number) based on l and the speed of light. Unfortunately, this does not answer our question what determined the dissipation rate. As we will see next, localized numerical simulations alone can only yield a partial answer to this question.

The magnetosphere can in principle establish a CKF-type equilibrium with a dissipationless current sheet, where all magnetic field lines that cross the light cylinder open up to infinity. In practice, localized numerical simulations have shown that, even without external driving, such a current sheet becomes unstable to relativistic Petschek reconnection (Sironi *et al.* 2013). A finite reconnection speed $v_{\rm converge} \sim 0.1c$ is established which corresponds to the maximum possible inflow speed for that particular type of reconnection, namely $v_{\rm maxPetschek} \approx (\pi/8 \ln \mathcal{R}_{\rm m})c$ (i.e. the reconnection electric field is practically independent of the local conditions in the current sheet; see e.g. Cowley 1985). This is a local property of the current sheet, and in that case a global magnetospheric configuration establishes itself such that $v^2_{\rm converge} + v^2_{\parallel \rm CS} \approx c^2$, or equivalently

$$B_r/B_z \sim 9.95 \tag{2.4}$$

right above and below the equatorial current sheet. Here, $v_{\parallel \rm CS} \equiv (E_{\perp \rm CS}/B_{\parallel \rm CS})c$ is defined as the drift velocity parallel to the current sheet just above and below it. As estimated in Eq. (2.4), the entry angle of magnetic field lines into the equatorial current sheet is very small, hence only a small amount of magnetospheric Poynting flux enters and is dissipated into the current sheet.

Another way to understand this configuration is to consider the analogy with an infinite infinitely thin plane conductor threaded by a uniform current distribution. In that case, a topology of uniform and opposite direction magnetic field $B_\parallel$ forms above and below the plane. The source of the field is the current sheet electric current. If we remove all external power sources and consider that the sheet is a non-ideal conductor with effective dissipation η, then the current will begin to die out, the current sheet will absorb electromagnetic energy from above and below, and the electric current will continue to flow as long as the magnetic field reservoir is not depleted (i.e. as long as there exist a

magnetic field above and below the plane). In that case, the driver of magnetospheric dissipation is the local dissipation rate in the equatorial current sheet.

We are a little concerned here that Petschek-type reconnection cannot proceed for too long. As is seen in numerical simulations, closed magnetic field islands form along the current sheet, and when the whole current sheet layer is filled with such islands, the process of tearing and island formation will not proceed any longer and that particular type of reconnection will saturate. This does not preclude of course the occurence of random strong localized energetic reconnection events along the current sheet which may yield powerful flashes of high-energy and/or radio emission (Cerutti *et al.* 2013, 2014). If our concern is justified then, however exciting the results of localized current sheet PIC numerical simulations may be, they do not represent what really goes on in steady state in the pulsar magnetosphere. In fact the latest 'ab initio' global magnetospheric simulations yield values of $B_r/B_\perp$ much smaller than 9.95 (on the order of unity near the light cylinder).

On the other hand, there is strong indirect evidence that strong dissipation *does* take place in the current sheet (e.g. Cerutti *et al.* 2015*b*; Kalapotharakos *et al.* 2014; Gruzinov 2014). So, how is the current sheet forced and how much? PIC numerical simulations do help, provided we have a clearer idea of how to interpret them. So, let us now consider an important feature of the equatorial current sheet, the so called Y-point, that may hold the answer to its vertical forcing.

3. The Y-point

Current sheets have a thickness comparable to the gyro-radius of the particles that support their electric current. It is well known that these particles follow meandering (snake) orbits and if a reconnecting electric field exists along the current sheet (i.e. if there is dissipation), these particles are accelerated along the direction of $E_{\parallel \mathrm{CS}}$ following Spiser orbits, i.e. meandering orbits that become narrower accross and more stretched along the direction of acceleration. In the particular case of the pulsar equatorial current sheet this is true only for the main charge carrier of the current sheet, the one with the sign of charge of the charged sheet. This charge carrier is accelerated outwards. The other charge carrier is accelerated inwards, but in doing so it meanders all the way to the outskirts (the surfaces) of the current sheet where the main $\mathbf{E} \times \mathbf{B}$ direction is still outwards. So, the meandering of the other charge carrier is 'messy', with excursions outside the current sheet. Nevertheless, on average, these too are accelerated inwards. However, it could be that they cannot survive for much time along the current sheet. This has already been seen in numerical simulations (Contopoulos 2007*b*; Philippov *et al.* 2015), and remains to be confirmed with further studies.

The particle gyro-radius is determined by the particle kinetic energy perpendicular to the magnetic field. In the pulsar magnetosphere, the perpendicular kinetic energy is quickly radiated away through curvature radiation, and if most of the kinetic energy is radiated away, then the particle gyro-radius becomes smaller and smaller, and the current sheet narrower and narrower. In the limit of very small gyro-radius the current sheet can still be held from collapsing by its own electrostatic repulsion (see Contopoulos *et al.* 2014, for details). In other words, the current sheet will never completely collapse because it is held by its own electrostatic repulsion. This is true unless we sit right at the Y-point.

As we have argued before, the poloidal magnetic field, thus also the poloidal electric field and the electric charge density all three vanish right outside (but not inside) the Y-point. It becomes then extremelly problematic to support a current sheet right outside

the Y-point, unless of course the external magnetic pressure (i.e. B_ϕ) also vanishes at that point! This simple result has very strong implications for the global structure of the magnetosphere. Firstly, this is equivalent to the vanishing of the electric current along the separatrix between the corotating dead zone and the open magnetosphere. There is no current sheet that returns to the star. The equatorial current sheet does not close the electric circuit onto the star. And if we do not allow for electric currents to flow through the Y-point, then the old CKF-type solution cannot be valid anymore, and the magnetosphere must find a new global equilibrium that is *different* from the CKF solution. In fact, we expect this equilibrium to be strongly dissipative in the current sheet for a simple reason: CKF argued that their solution is the only possible solution for a dissipantionless ideal magnetosphere. The new solution is still ideal everywhere, but very different in the current sheet, thus also strongly dissipative there. The equatorial current sheet must be gradually replenished by the magnetospheric electric charges that both support it vertically and also form the electric current that threads it. In doing so, Poynting flux enters the current sheet, and this energy flux must find a way to dissipate in the current sheet through reconnection and particle acceleration (with ensuing emission of radiation). We have thus found the origin of the magnetospheric forcing of the current sheet, namely the inability of the electric current in the current sheet to cross the Y-point.

The magnetospheric Y-point is indeed a problematic place and several authors have studied it in detail in the past. It cannot approach too close to the light cylinder because in that case the corotation velocity at the tip of the dead zone would approach the speed of light and the magnetic and electric fields right inside it would diverge (Uzdensky 2003). At the same time, it must be in a position to support a sudden drop in its charge density. We will now present why we believe it is hard in practice for the Y-point to also support a continuous electric current through it. Before we proceed, let us here define as the 'right' type of particles, those that, when they move outwards, they support the magnetospheric electric current, and 'wrong' the other type. For example, in the case of the equatorial current sheet in the aligned rotator (Ω parallel to the magnetic moment of the star), the positrons/protons/ions are of the 'right' type, and electrons of the 'wrong' one.

In order to support at the same time a continuous current, a sudden density drop across, and a zero charge density just outside the Y-point, we must have two populations of particles that satisfy both

$$\rho_{\rm wrong} + \rho_{\rm right} = 0 \ , \ \text{and} \tag{3.1}$$

$$\rho_{\rm wrong} v_{\rm wrong} + \rho_{\rm right} v_{\rm right} = J_{\rm Y} \ . \tag{3.2}$$

However small the amount of dissipation in the equatorial current sheet (i.e. even if we just have spontaneous relativistic Petschek-type reconnection as shown in the localized numerical simulations of Sironi *et al.* 2013), then its electric field accelerates particles of the wrong type inwards. Therefore $v_{\rm wrong}$ is inward and particles of the wrong sign must follow *inward* meandering (snake) orbits traveling from outside the light cylinder into the Y-point. Unfortunately, this is not allowed topologically in a 3D magnetosphere (i.e. oblique rotator) for the following reason: outward moving particles of the right type do support a trailing (retarded) spiral current sheet (in the shape of a spinning balarina skirt). Outside the light cylinder, particles cannot move inwards along such a 3D current sheet, thus $\rho_{\rm wrong}$ must vanish outside the light cylinder. According to eq. (3.2) $J_{\rm Y}$ must also vanish there.

We are thus left with one possibility, namely a strongly dissipative equatorial current sheet with no electric current at the Y-point. This is the new standard magnetosphere of Contopoulos *et al.* (2014). We plan to investigate this solution in greater detail in the

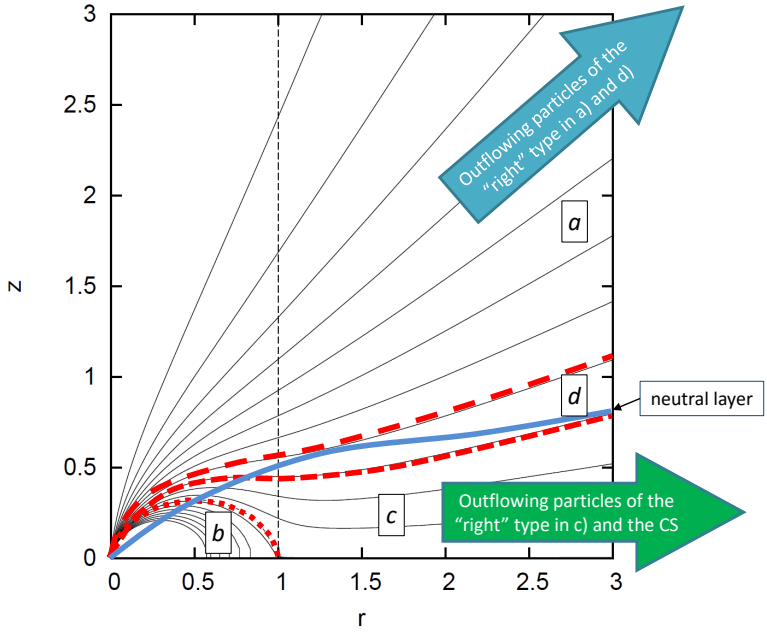

FIGURE 2. The crossings of the null surface in the standard ideal force-free axisymmetric CKF magnetosphere. Vertical dashed line: the light cylinder. Blue line: null line (the neutral layer). The three red lines separate the four types of field lines (see text for details). Type a: above red long dashed line. Type b: below red dotted line. Type c: between red dotted and short dashed lines. Type d: between red short and long dashed lines. The red short dashed line is the line of zero poloidal electric current $J_{\rm CKF}$ (the electric current null line) that separates the magnetosphere into two regions of outgoing and ingoing electric currents respectively. For example, in the case of aligned pulsars, the 'right' type of particles are outflowing electrons in regions a) and d) (large blue arrow), and outflowing protons or positrons in region c) and in the equatorial current sheet (CS; large green arrow). The electric charge and electric current null lines become one asymptotically (as $r \to \infty$).

future. Meanwhile, let us go back to the old standard magnetosphere (CKF) and discuss certain of its features that have not been properly emphasized in the literature.

4. The crossings of the null surface

In the old standard magnetosphere, there is a line (in 3D a surface) along which the Goldreich-Julian space charge density vanishes. This is the so called null line (or null surface in 3D). In relation to the null line, there are four types of field lines (see Fig. 2):

(a) Open field lines that do not cross the null line. These originate on the stellar polar cap around the magnetic axis (which in axisymmetry coincides with the axis of rotation), and carry the main part of the polar cap poloidal electric current.

(b) Closed field lines. All of them do cross the null line. These originate at low stellar latitudes up to the polar cap, and do not carry any poloidal electric current.

(c) Open field lines that cross the null line once. These originate at the outskirts of the polar cap, and carry some fraction of the return poloidal electric current.

(d) Open field lines that cross the null line twice. These originate somewhere inside the polar cap, and carry a very small amount of electric current of the same polarity as the main part of the polar cap.

Let us now consider each field line category and propose how it may be filled with charged particles. Notice that the source of particles may very well be a stellar reservoir of protons (ions) and electrons, and does not need to resort to pair formation in magnetospheric gaps.

The first type of field lines can very well be filled *only with one* type of particles, the one that we call 'right'. In this part of the magnetosphere, the 'right' type can perfectly accommodate both the charge and electric current, namely $\rho = \rho_{\rm GJ}$ everywhere (in fact almost everywhere as we will see next), and $J_{\rm CKF} = \rho_{\rm GJ} v_{\rm poloidal}$. Following our definition of $J_{\rm CKF}$ and $J_{\rm GJ}$ in § 1.2, one can easily check that

$$J_{\rm CKF} \ll J_{\rm GJ} \ , \tag{4.1}$$

near the stellar surface, and $J_{\rm CKF}$ flows in the same direction as $J_{\rm GJ}$, hence only one type of charge carrier is sufficient to accomodate both the charge and electric current densities by adjusting the value of $v_{\rm poloidal} \ll c$, and

$$J_{\rm CKF} \to J_{\rm GJ} \tag{4.2}$$

at large distances, where $v_{\rm poloidal} \to c$. There is nothing terribly interesting to discuss in this region. There is a slight complication at the outskirts of this region where field lines at some point approach close to the null line, and at those positions the adjustment of $v_{\rm poloidal} \equiv J_{\rm CKF}/\rho_{\rm GJ}$ does not work because the flow would become superluminal, but we will discuss this in relation to the field lines of the fourth type as defined above.

The second type of field lines does not have any problem whatsoever to be filled with two types of particles, positive and negative, that simply corotate with the star and thus form the so called dead zone. Nothing is moving in the poloidal direction, and the poloidal electric current is zero. The particles are held in corotation by microscopic electric forces that are outside the realm of numerical ideal MHD analysis.

The third type of field lines is much more interesting. These field lines start with the 'wrong' type of charge carriers on the stellar surface, and switch to the 'right' type beyond the null surface. Asymptotically, Eq. (4.2) still holds where $v_{\rm poloidal} \to c$. So these field lines need to *at least* carry just the Goldreich-Julian charge density at large distances. These particles of the 'right' type can very well originate on the stellar surface and support the electric current all the way to the star. What needs to be done is to also pull the right amount of 'wrong' type particles from the stellar surface in order just to fill the region from the stellar surface up to the null line and some small distance beyond. In a configuration with the *minimal possible number of particles*, the innermost part of the third type of field lines contains a corotating region of the 'wrong' type of particles with density

$$\rho_{\rm corotating} \approx \rho_{\rm GJ} - \frac{J_{\rm CKF}}{c} \ . \tag{4.3}$$

Obviously, since $\rho_{\rm GJ}$ becomes zero some distance downstream along these lines, the corotating region of the 'wrong' type particles must extend some distance further downstream from the null line. We suspect that the region of corotating charge never extends beyond the light cylinder (where corotation is obviously not supported), and this is helped by the fact that $J_{\rm CKF} \to 0$ at the boundary between regions three and four.

The fourth type of field lines is the most interesting of all. These carry an electric current which can very well be accommodated only by charge carriers of the 'right' type (which is the same type as the 'right' type for region one) since $J_{\rm CKF} \to J_{\rm GJ}$ at large distances, but consists of three regions of electric charge, of the 'right' type near the star and at very large distances, and of the 'wrong' type in between. The most economical obvious way to satisfy all the requirements in this region is to increase the number density of particles of the 'right' type, and add a population of outflowing particles of the 'wrong' type which will adjust their poloidal velocities in order to build the in between region of the 'wrong' type Goldreich-Julian density. This configuration will extend also to the

outskirts of region one in order to avoid superluminal velocities for particles of the 'right' type.

In any case, the poloidal speed of the charge carriers of the 'wrong' type will be much smaller than the speed of the charge carriers of the 'right' type. Thus, in regions three and four (extended also to the outskirts of region one), it is very natural to expect a configuration where a population of relativistic $v \approx c$ particles of one type flows through a large population of almost stationary particles of the other type. Such a configuration may naturally yield Cherenkov type instabilities that may be related to the pulsar radio emission, as discussed e.g. in Lyutikov *et al.* (1999). This scenario certainly merits further investigation.

5. Epilogue

We have constructed a very economical pulsar magnetosphere consisting of large corotating regions filled with particles of one type of charge, threaded by streams of fast outflowing particles of the other type of charge. It is thus possible to fill the magnetosphere with a minimum amount of charge carriers by adjusting their speed and concentration that does not require continuous pair formation in the magnetosphere. In fact, particles of both negative and positive charge can naturally be found in the neutron star atmosphere with no need to resort to pair formation. Nature manages its resources wisely, so, instead of spending energy to produce a multitude of pairs, it can fill the magnetosphere with protons and electrons provided freely by the star. In that case, aligned rotators will obviously differ from counter-aligned ones. In particular, the equatorial current sheet of aligned pulsars will contain protons which will produce a markedly different high energy signature than that of counter-aligned pulsars which contains electrons. Moreover, aligned pulsars will contain large corotating regions filled with electrons which may also produce a radio signal different from that of counter-aligned pulsars. Future observations may indeed be able to discriminate between aligned and counter-aligned pulsars.

We have also emphasized certain restrictions in the equatorial current sheet that may prevent it from extending all the way to the stellar surface. The latter dramatically modify the structure of the pulsar magnetosphere away from the standard ideal MHD solution. Obtaining the new standard solution required the investigation of several magnetospheric issues in detail that cannot be reached in modern state-of-the-art 3D numerical simulations. The most recent numerical simulations yield vague hints that the magnetospheric structure is closer to the new standard solution, but are not yet in a position to reveal its details. We believe that it is too early to run global 'ab initio' magnetospheric PIC simulations since we need to understand in greater depth how the local conditions around the current sheet affect the global magnetospheric structure. Therefore, what we propose instead is to focus future PIC simulations in the study of the equatorial current sheet and the Y-point, and combine them with ideal MHD/FFE simulations of the global magnetosphere.

Our numerical simulations were performed using the resources of the NRNU MEPhI High-Performance Computing Center.

REFERENCES

Baker, J. G., Giacomazzo, B., Kanner, J., Kelly, B. J. & Schnittman, J. 2013 Electromagnetic Counterparts to Supermassive Black Hole Mergers. In *AAS/High Energy Astrophysics Division*, *AAS/High Energy Astrophysics Division*, vol. 13, p. 121.01.

Beskin, V. S. 2010 *MHD Flows in Compact Astrophysical Objects*.

Cerutti, B., Philippov, A., Parfrey, K. & Spitkovsky, A. 2015*a* Particle acceleration in axisymmetric pulsar current sheets. *Mon. Not. Roy. Astron. Soc.* **448**, 606–619.

Cerutti, B., Philippov, A. A. & Spitkovsky, A. 2015*b* Modeling high-energy pulsar lightcurves from first principles. *ArXiv e-prints* .

Cerutti, B., Werner, G. R., Uzdensky, D. A. & Begelman, M. C. 2013 Simulations of Particle Acceleration beyond the Classical Synchrotron Burnoff Limit in Magnetic Reconnection: An Explanation of the Crab Flares. *Astrophys. J.* **770**, 147.

Cerutti, B., Werner, G. R., Uzdensky, D. A. & Begelman, M. C. 2014 Three-dimensional Relativistic Pair Plasma Reconnection with Radiative Feedback in the Crab Nebula. *Astrophys. J.* **782**, 104.

Chen, A. Y. & Beloborodov, A. M. 2014 Electrodynamics of Axisymmetric Pulsar Magnetosphere with Electron-Positron Discharge: A Numerical Experiment. *Astrophys. J. Lett.* **795**, L22.

Contopoulos, I. 2005 The coughing pulsar magnetosphere. *Astron. Astrophys.* **442**, 579–586.

Contopoulos, I. 2007*a* A note on the cyclic evolution of the pulsar magnetosphere. *Astron. Astrophys.* **475**, 639–642.

Contopoulos, I. 2007*b* The magnetic field topology in the reconnecting pulsar magnetosphere. *Astron. Astrophys.* **472**, 219–223.

Contopoulos, I. 2007*c* The role of reconnection in the pulsar magnetosphere. *Astron. Astrophys.* **466**, 301–307.

Contopoulos, I. & Kalapotharakos, C. 2010 The pulsar synchrotron in 3D: curvature radiation. *Mon. Not. Roy. Astron. Soc.* **404**, 767–778.

Contopoulos, I., Kalapotharakos, C. & Kazanas, D. 2014 A New Standard Pulsar Magnetosphere. *Astrophys. J.* **781**, 46.

Contopoulos, I., Kazanas, D. & Fendt, C. 1999 The Axisymmetric Pulsar Magnetosphere. *Astrophys. J.* **511**, 351–358.

Cowley, S. W. H. 1985 Magnetic reconnection. In *Solar System Magnetic Fields* (ed. E. R. Priest), pp. 121–155.

Goldreich, P. & Julian, W. H. 1969 Pulsar Electrodynamics. *Astrophys. J.* **157**, 869.

Gruzinov, A. 2013 Aristotelian Electrodynamics solves the Pulsar: Lower Efficiency of Strong Pulsars. *ArXiv e-prints* .

Gruzinov, A. 2014 How Pulsars Shine: Poynting Flux Annihilation. *ArXiv e-prints* .

Kalapotharakos, C. & Contopoulos, I. 2009 Three-dimensional numerical simulations of the pulsar magnetosphere: preliminary results. *Astron. Astrophys.* **496**, 495–502.

Kalapotharakos, C., Contopoulos, I. & Kazanas, D. 2012 The extended pulsar magnetosphere. *Mon. Not. Roy. Astron. Soc.* **420**, 2793–2798.

Kalapotharakos, C., Harding, A. K. & Kazanas, D. 2014 Gamma-Ray Emission in Dissipative Pulsar Magnetospheres: From Theory to Fermi Observations. *Astrophys. J.* **793**, 97.

Kundt, W. 1998 Astrophysics of Neutron Stars - Facts and Fiction about their Formation and Functioning. *Fundamenals Cosm. Phys.* **20**, 1–119.

Lovelace, R. V. E., Turner, L. & Romanova, M. M. 2006 Jets and Disk Winds from Pulsar Magnetospheres. *Astrophys. J.* **652**, 1494–1498.

Lyubarskii, Y. E. 1990 Equilibrium of the Return Current Sheet and the Structure of the Pulsar Magnetosphere. *Soviet Astronomy Letters* **16**, 16.

Lyubarsky, Y. & Kirk, J. G. 2001 Reconnection in a Striped Pulsar Wind. *Astrophys. J.* **547**, 437–448.

Lyutikov, M., Machabeli, G. & Blandford, R. 1999 Cherenkov-Curvature Radiation and Pulsar Radio Emission Generation. *Astrophys. J.* **512**, 804–826.

McKinney, J. C. 2006 Relativistic force-free electrodynamic simulations of neutron star magnetospheres. *Mon. Not. Roy. Astron. Soc.* **368**, L30–L34.

Ogura, J. & Kojima, Y. 2003 Some Properties of an Axisymmetric Pulsar Magnetosphere Constructed by Numerical Calculation. *Progress of Theoretical Physics* **109**, 619–630.

Philippov, A. A., Spitkovsky, A. & Cerutti, B. 2015 Ab Initio Pulsar Magnetosphere: Three-dimensional Particle-in-cell Simulations of Oblique Pulsars. *Astrophys. J. Lett.* **801**, L19.

Ponce, M., Palenzuela, C., Lehner, L. & Liebling, S. L. 2014 Interaction of misaligned magnetospheres in the coalescence of binary neutron stars. *Phys. Rev. D* **90** (4), 044007.

Sironi, L., Spitkovsky, A. & Arons, J. 2013 The Maximum Energy of Accelerated Particles in Relativistic Collisionless Shocks. *Astrophys. J.* **771**, 54.

Spitkovsky, A. 2006 Time-dependent Force-free Pulsar Magnetospheres: Axisymmetric and Oblique Rotators. *Astrophys. J. Lett.* **648**, L51–L54.

Tchekhovskoy, A., Spitkovsky, A. & Li, J. G. 2013 Time-dependent 3D magnetohydrodynamic pulsar magnetospheres: oblique rotators. *Mon. Not. Roy. Astron. Soc.* **435**, L1–L5.

Timokhin, A. N. 2006 On the force-free magnetosphere of an aligned rotator. *Mon. Not. Roy. Astron. Soc.* **368**, 1055–1072.

Uzdensky, D. A. 2003 On the Axisymmetric Force-free Pulsar Magnetosphere. *Astrophys. J.* **598**, 446–457.